COUPLING CELL MOVEMENT TO MULTICELLULAR DEVELOPMENT IN MYXOBACTERIA

Dale Kaiser

The myxobacteria are Gram-negative organisms that are capable of multicellular, social behaviour. In the presence of nutrients, swarms of myxobacteria feed cooperatively by sharing extracellular digestive enzymes, and can prey on other bacteria. When the food supply runs low, they initiate a complex developmental programme that culminates in the production of a fruiting body. Myxobacteria move by gliding and have two, polarly positioned engines to control their motility. The two engines undergo coordinated reversals, and changes in the reversal frequency and speed are responsible for the different patterns of movement that are seen during development. The myxobacteria communicate with each other and coordinate their movements through a cell-contact-dependent signal. Here, the cell movements that culminate in the development of the multicellular fruiting body are reviewed.

SPORANGIUM
A specialized structure that contains myxobacterial spores.

TRANSDUCTION
The virus-mediated transfer of host DNA (plasmid or chromosomal) from a donor cell to a recipient cell.

TRANSFECTION
The transformation of prokaryotic cells with viral DNA or RNA.

Stanford University, Departments of Biochemistry and Developmental Biology, Stanford, California 94305, USA.
e-mail: kaiser@cmgm2.stanford.edu
doi:10.1038/nrmicro733

Myxobacteria are voluntary multicellular microorganisms that are common in the topsoil. Given a nutritionally complete liquid medium, these Gram-negative bacteria grow as independent cells. However, when in contact with each other on a solid medium, such as nutrient agar, they interact and grow as a swarm that spreads indefinitely outwards from the point of inoculation to gain access to nutrients in the agar. The cells feed cooperatively by pooling their extracellular digestive enzymes[1,2]. Myxobacteria can prey on other bacteria by surrounding a colony, lysing the cells with lysozyme, digesting the released proteins, lipids and nucleic acids, and sharing the proceeds. When the available food runs low, they stop swarming outwards and instead congregate at foci where they build fruiting bodies.

Myxobacterial fruiting bodies each comprise ~10^5 cells and are constructed through coordinated movements. The overall shape of a fruiting body is species specific. Some fruiting bodies, such as those of *Myxococcus xanthus*, *Myxococcus virescens* and *Myxococcus fulvus*, consist of a spherical SPORANGIUM resting on a short stalk. *Myxococcus stipitatis* elevates the sporangium on a tall stalk, whereas *Stigmatella aurantiaca* and *Chondromyces* spp. create thick stalks topped with several sporangioles[3]. When they have completed the building movements, cells within the sporangium of the fruiting body differentiate to become heat-resistant spores, and the spores are subsequently dispersed (BOX 1).

The experimental genetics of myxobacteria began in 1970, with the isolation of motility mutants of *M. xanthus*[4]. Soon, classical microbial genetic-transfer methods — TRANSDUCTION, DNA TRANSFECTION and transposon insertion — were used to map and construct strains[5]. Complementation experiments revealed that *M. xanthus* passes several signals between its cells to initiate and coordinate a programme of fruiting-body development and spore differentiation[6]. Two chemical signals — the diffusible A-signal and the cell-bound C-signal — were identified[7–10]. According to a proposed developmental regulatory circuit, the shape of the *M. xanthus* fruiting body and the location of its spores depends on the C-signal[11,12]. Cell movement brings cells into close contact, and end-to-end contact between two cells enables them to transmit the C-signal to each

Box 1 | Proposed developmental cycle for myxobacteria

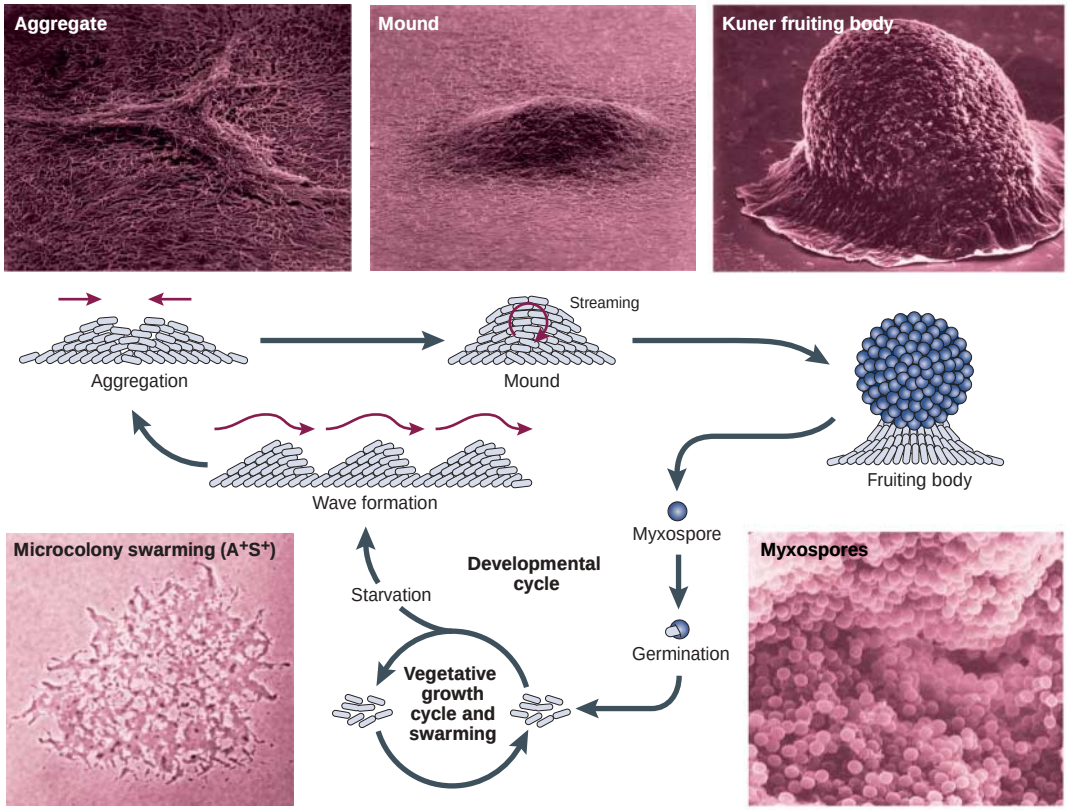

During vegetative growth, myxobacteria form multicellular swarms that feed cooperatively, and that can prey on other bacteria as a nutrient source (microcolony swarming). Under starvation conditions however, the myxobacteria initiate a complex developmental cycle to sporulate, during which they use a cell-contact-dependent signal (the C-signal) to coordinate their movements. I would like to propose the following scheme for the *Myxococcus xanthus* developmental cycle, which is in line with experimental observations. The first organized pattern of movement that is seen in a developing myxococcal culture is the appearance of organized waves of cells. If two waves of cells travelling in opposite directions collide at an area of high-cell density at the culture edge, then the cells are effectively in a 'traffic jam' and stationary aggregates of cells are formed (aggregate). Meanwhile, travelling waves of cells will wash over the aggregates, both depositing and removing cells; consequently, some aggregates increase in size whereas others can shrink and disappear altogether. In a submerged agar culture system, the aggregates can be stationary for a long period of time then suddenly, adjacent aggregates that are less than one wavelength apart begin to fuse together to form larger mounds of cells. Fusion is spontaneous, but at present, its mechanism is unknown. At this time in the developmental cycle, the cells in the aggregates become motile again, and are streaming in cycles within the mounds. As the mounds increase in size they eventually form fruiting bodies, which can contain up to 10^5 cells. Streaming cells in the mounds have many end-to-end contacts with each other, and the C-signal is transmitted with each contact. Through the positive feedback mechanism discussed in the text, the number of C-signal molecules on the cell surface increases, eventually reaching the threshold that is required for sporulation. In agreement with this mechanism, only cells inside the fruiting body are capable of becoming myxospores. When nutrients become available, the myxospores germinate, and the vegetative growth cycle begins again. Micrographs are reproduced with permission from REFS 15,59 © (1979, 1982) Springer–Verlag and American Society for Microbiology, respectively.

other[13]. Recent genetic studies have been facilitated by the availability of gene sequences, and completion of the 9.1-Mb genome sequence of *M. xanthus* is scheduled for the end of 2003 (see TIGR in Online links).

Gliding motility: two engines

Cell movement on surfaces is necessary for swarming and fruiting-body development. To move on surfaces, including the surfaces of their sibling cells, myxobacteria use gliding motility, as they have no flagella and are unable to swim. Social gliding is closely related to twitching, and both depend on TYPE IV PILI (BOX 2). Microscopically, gliding is a smooth movement without rotation, in the direction of the long axis of the cell[14]. From time to time, gliding cells stop and reverse direction. To reverse, they seldom make 'U-turns'; instead, they undergo a reversal of polarity in which the head becomes the tail, and the tail the head (see Online Movie).

The isolation of motility mutants[15,16] revealed that there are two different gliding engines, referred to as

TYPE IV PILI
Elongated hair-like structures extending from the surface of Gram-negative cells that are independent of flagella, and which can retract and pull the cell forward.

AAA MOTOR PROTEIN
An ATPase that is associated with various cellular activities. AAA proteins are essential in all organisms.

Box 2 | Gliding motility, twitching motility and type IV pili

Twitching motility has been described by Henrichsen as an intermittent and jerky movement, predominantly of single Gram-negative cells, which is independent of flagella[68]. Henrichsen found that the many twitching strains in his collection always had pili[69]; these pili were subsequently recognized as type IV pili. Henrichsen also distinguished twitching from gliding; he described the latter as smooth movement in the direction of the long axis of the cell[68]. Despite the difference in the types of movement, genetic experiments of the past 25 years with both the twitching *Pseudomonas aeruginosa* and *Neisseria gonorrhoeae*, and the gliding *Myxococcus xanthus*, have shown that the same set of type IV pilus genes is essential for cell movement, thereby indicating that gliding and twitching have a common mechanism. The extensive data on type IV pilus structure, and assembly and retraction relating to twitching have been reviewed[70]. The different presentation of twitching and gliding probably results from differences in the viscosity of the fluid in which the cells move. Cells surrounded by a fluid of low viscosity twitch, whereas the high viscosity of secreted slime would account for the smooth movement of gliding in *M. xanthus*.

M. xanthus is a favourable organism for genetic studies of social-gliding motility and type IV pilus biogenesis because its 17 *pil* genes are conveniently clustered[28], and because the edge of an S-motile swarm of *Myxococcus* can be seen with the naked eye. So, non-motile mutants can be identified without the use of a microscope[15,16]. The genes required for retraction and reversal have been identified within the *pil* cluster. With few exceptions, the *pil* genes of *M. xanthus* are homologues of genes in *P. aeruginosa* and *N. gonorrhoeae* that support the twitching motility necessary for the virulence of these pathogens[71,72], but are less clustered. Like S-motility in *M. xanthus*, twitching in *P. aeruginosa* gives rise to the organized spreading of a swarm with cell reversal[70], and requires pilus retraction[24]. Twitching also supports the spreading of a biofilm[73]. The parallels with *M. xanthus* raise the question whether *P. aeruginosa* pili switch polarity from one cell end to the other to reverse their direction of cell movement and, if so, how those reversals are controlled. *P. aeruginosa* does have a complete *frizzy*-like chemosensory set of genes, which controls its twitching motility, and therefore might be part of a pathway for reversal control[70].

engine A and engine S, which normally cooperate with each other. Hodgkin found roughly equal numbers of mutants that lacked either engine A or engine S[15,16], and he distinguished them by their different swarm patterns (FIG. 1). In A^+S^+ cells, both gliding engines are present and the elimination of any gene that is essential for one engine results in a swarm pattern that is characteristic of the remaining engine. In a swarm of A^+S^- cells, individual cells, as well as clusters, are evident at the swarm edge (FIG. 1b). The ability of lone cells to move led Hodgkin to name this pattern A, for adventurous[16]. In fact, most A^+S^- cells are found strung out in side-by-side clusters (FIG. 1b). By contrast, in a swarm of A^-S^+ cells, there are almost no single cells at the swarm edge. Instead, cells are found clustered in stubby peninsulas and in rafts of 20–50 cells, leading Hodgkin to name this pattern S, for social (FIG. 1a). A^-S^- cells are unable to swarm or form fruiting bodies.

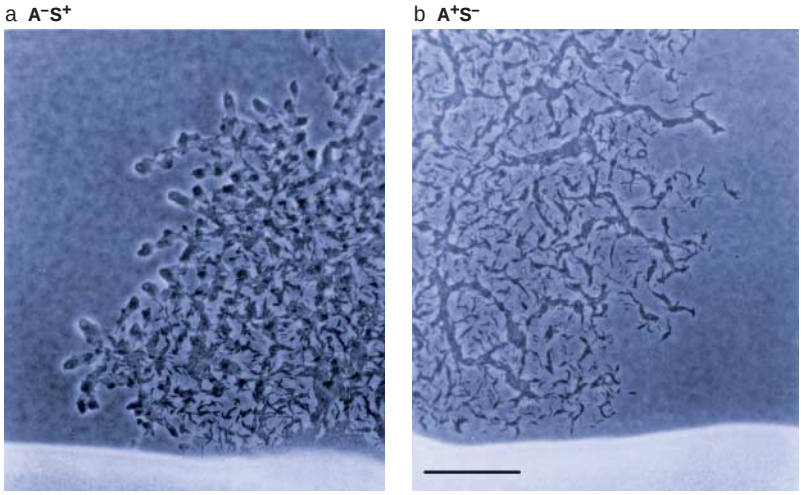

Figure 1 | **The swarm edges of an A^-S^+ strain and an A^+S^- strain. a** | Shows the A^-S^+ strain. **b** | Shows the A^+S^- strain. Some individual cells, which are 0.5 x 5–7 μm rods, can be seen at the outside edge of the A^+S^- swarm. The scale bar is 50 μm. Reproduced with permission from REF. 16 © (1979) Springer–Verlag.

S-motility: pili production and fibrils

S^+ cells, whether A^- or A^+, have type IV pili, and S-motility arises from the retraction of one or more of these pili, which extend forward from the head of the cell[17] (FIG. 2). These pili are long, thin (6-nm diameter) hair-like structures, often several times as long as a *Myxococcus* cell, and are unipolar organelles — only 5% of cells have pili at both poles[18]. The pilus filament comprises a single protein, PilA[19]; another ten Pil proteins are assembled in the inner membrane, and other Pil proteins provide a gated channel through the outer membrane[20].

PilT is one of the inner-membrane proteins and is an AAA MOTOR PROTEIN[21,22]. *pilT* mutants lack S-motility but retain pili. Using laser tweezers, Merz, So and Sheetz directly measured a retractile force of 80 pN from a single type IV pilus in *Neisseria gonorrhoeae*[23]. Pilus retraction is believed to involve disassembly of the helical array of pilin subunits. The observed retraction rate of 1.2 μm s^{-1} implies the removal of ~1,500 pilin subunits each second from the base of the fibre[24]. Evidence in *M. xanthus* indicates that PilT is important in catalysing pilus retraction[25,26]. *M. xanthus* shares a pilus retraction mechanism with many other bacteria that have type IV pili, such as *N. gonorrhoeae*[21] and *Pseudomonas aeruginosa*, in which the retraction and extension processes have been studied extensively[27]. The pilus protein composition of *Myxococcus*, *Neisseria* and *Pseudomonas* is almost identical (REF. 28; E. Nudleman, unpublished observations).

Like the *pilT* mutants, another group of S^- mutants — the *dsp* (dispersed growth) mutants — have pili but nevertheless lack S-motility. These mutants lack

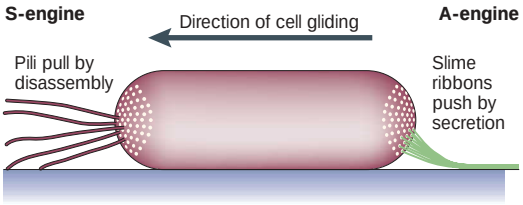

Figure 2 | **The two engines of myxobacteria.** Both engines are unipolar, multi-protein devices. The slime-secreting A-engine is a 'pusher', whereas the pilus-retracting S-engine is a 'puller'. The high rate of A^+S^+ swarm expansion indicates that when a cell reverses, both engines coordinately move to their opposite poles. Slime-secretion pores are always visible at both ends of each cell, and yet only one end secretes slime[40]. Similarly, many of the basal pilus proteins are present at both cell ends, but pili are assembled at only one end[18]. In the case of pili, it has been shown that, at any instant, only one end has the Tgl lipoprotein, a necessary pilus-assembly factor (E. Nudleman, manuscript in preparation).

FIBRILS[29–31], which consist of almost equal amounts of the monosaccharides galactose, glucosamine, glucose, rhamnose and xylose, and several proteins, which can be distinguished by their antigens. The fibrils are linked together in a network that joins neighbouring cells in a cluster[32,33]. S-motility is not observed among cells that are more than one pilus-length apart[34]. Together, these observations indicate that the pilus extends ahead of an *M. xanthus* cell, adheres to the fibrils on the cells ahead of it and then retracts, pulling the leading end of the piliated cell forward.

Bowden and Kaplan have reported that mutants defective in lipopolysaccharide (LPS) O-ANTIGEN biosynthesis lack S-motility, but do have pili[35]. These LPS mutants have many more pilus filaments than are found in wild-type cells. In a separate study, it was shown that *M. xanthus pilT* mutants that also lack fibrils have more pili than wild-type cells because the pili do not retract; additionally, it was shown that the addition of fibril material rescued the mutants[36]. Bowden and Kaplan's data could be explained if the O-antigen mutants are also deficient in pilus retraction. This explanation is plausible because chains of the O-antigen completely cover the cell surface. As a retracting pilus slides through this covering, it would interact repeatedly with the O-antigen chains.

A-motility: slime production

Gliding myxobacteria leave a trail of slime behind them on the agar surface, which is thought to indicate the mechanism of A-motility. FIG. 3 shows a magnified view (relative to FIG. 1) of the edge of an A^+S^- swarm. Each cell has left a slime trail, evident as a phase-bright line. Clusters of cells leave a wide trail and single cells leave a narrow trail. In several time-lapse motion-picture series, Reichenbach first showed that myxobacteria tend to follow a pre-existing trail (see REFS 37,38 for examples). When a cell begins to cross an existing trail, it turns, probably through the acute angle of intersection, to follow the trail. Cells are often observed to move in both directions on the same trail. Owing to its stickiness, myxococcal slime has proved difficult to isolate, but some A^- mutants that can change the composition of a slime polysaccharide have recently been identified by transposon-insertion mutagenesis (R. Yu, unpublished observations). The fact that the trails are visible indicates that the slime trail has a different refractive index from that of 1% agar. Moreover, cell speed depends on the agar concentration[39]. Pili are not necessary to make a slime trail because the trails of a pili-less mutant look much like those of a wild-type strain[40].

Electron microscopy revealed the presence of more than 200 thick-walled rings clustered at both ends of *M. xanthus* cells, but only a few rings in the mid-section of the cells[40] (FIG. 4). These rings are thought to be the jets that are used for slime secretion, as they cannot be secretin complexes because they are present in *pilQ* deletion mutants[40], and they resemble the junctional pore complexes that are used to secrete propulsive slime by the cyanobacterium *Phormidium uncinatum*[40,41]. Several elementary strands of slime are secreted through each of these rings, which associate laterally to form ribbons of slime gel and are deposited as the slime trail. Although the rings are present at both ends of a cell, *in vivo* slime is seen emerging from only one end at a time[40] (FIGS 2,4), indicating that myxobacterial cells restrict their slime secretion to one end of the cell at a time.

Elasticotaxis. A^+S^+ cells swarm outwards rapidly from the edge of a colony, moving equally in all directions. Stanier discovered that, when swarming on stretched or compressed agar, the swarm disc becomes asymmetrically elongated[42] and he called this effect elasticotaxis. More recently, Fontes has shown that the A-engine is responsible for this asymmetry because elasticotaxis does not occur in an A^- mutant[43], and it has also been shown that elasticotaxis is diminished in a weak A^- mutant, in proportion to the decrease in the swarming rate (R. Yu, unpublished observations).

Fontes also linked elasticotaxis to the re-orientation of individual cells, which respond within minutes to the orientating effect of compressed agar[43]. It is attractive to think that gliding on compressed (or stretched) agar is

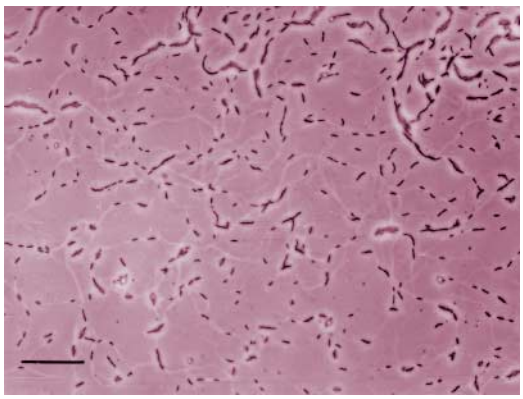

Figure 3 | **Slime trails at the edge of a *Myxococcus xanthus* A^+S^- swarm.** A side-by-side cluster of cells leaves a trail that is the same width as the cluster. Most *M. xanthus* cells are found near the middle of a trail, not at the end, indicating that these cells have reversed on the trail. The scale bar is 50 μm. A time-lapse movie shows cells reversing on their own trail (see Online Movie).

FIBRILS
Filamentous extracellular matrix material comprising polysaccharides and protein.

O-ANTIGEN
A heat-stable antigen that is associated with Gram-negative bacteria and which comprises chains of identical oligosaccharide units that can vary in length.

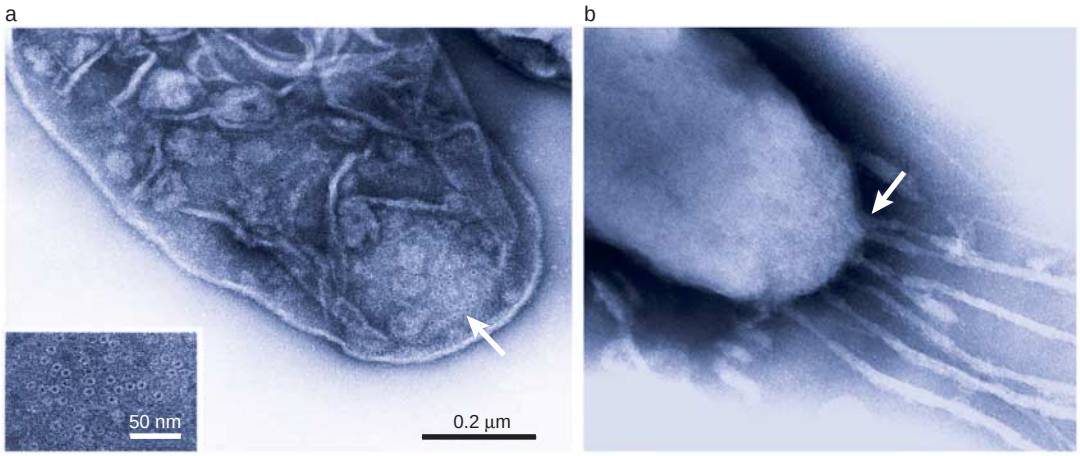

Figure 4 | **Electron micrograph of the sacculus of a *Myxococcus xanthus* cell. a** | The thick-walled rings (white arrow) near the end of the cell can be seen. The inset shows the rings at higher magnification; note the scale bar. Some 80% of the rings were found at the ends of cells; the remainder were found in the long mid-section. These rings are believed to be an end view of slime-secretion jets, as explained in REF. 40. **b** | An electron micrograph of a negatively stained cell showing the emergence of several ribbons of slime (white arrow). Reproduced with permission from REF. 40 © (2002) Elsevier Science.

much like following a slime trail, which would also help to explain why A-motile swarming is faster on concentrated agar than on dilute agar[39]. Oriented agarose chains in compressed agar, or oriented slime polymer chains in a trail, could have similar orientating effects on an A-motile cell. It is thought that cells turn onto a trail because this alignment maximizes the number of cohesive interactions between the filaments of its newly secreted slime and the filaments laid down earlier in the slime trail. Similar interactions might be expected to occur between the newly secreted slime and oriented agarose chains, and this is supported by the correlation between swarm rate and elasticotaxis.

Elasticotaxis helps myxobacteria locate bacterial colonies on which to feed. That *Myxococcus* detects, and swarms directly towards, a nearby colony of potential prey on which it can feed has been shown experimentally[44] (FIG. 5). When a *Myxococcus* swarm passes near the prey, a branch of the swarm is extended directly towards it. This directed extension had been observed earlier, and was initially interpreted as chemotaxis towards the prey. However, Dworkin showed that *Myxococcus* also extends a swarm branch directly towards a colony-sized plastic bead that contains no organic material and found that an A^- mutant failed to attack a colony or a bead, whereas an S^- mutant retained the ability to attack — paralleling the observations of Fontes (FIG. 5). Most likely, a colony of prey bacteria (or a bead) produces elastic stress in the gelatinous substratum on which the colony (or bead) rests, with stress lines radial to the colony. *Myxococcus* cells orient and move in the direction of these stress lines, so heading directly towards the prey colony.

Movement patterns: reversing the engines

The movement patterns of myxobacterial cells change during the developmental cycle. In the presence of nutrients, the bacteria swarm to facilitate cooperative feeding. At high cell density, in the absence of nutrients and on a solid surface, the bacteria undergo a programme of development that results in the formation of spore-filled fruiting bodies. At different stages of fruiting-body development, different patterns of organized cell movement, including wave formation and aggregation, are seen. *M. xanthus* cells move using gliding motility, and their movement is controlled by the two polar motility engines described earlier. The different patterns of cell movement are controlled by systematic regulation of the reversal of these motility engines.

Swarming. Swarming is a cooperative process, as shown by the fact that the swarm rate increases with increasing initial cell density, which indicates that individual cells help each other to move outwards. There is evidence that the two engines are located at opposite poles of the cell as the S-engine 'pulls' whereas the A-engine 'pushes' (FIG. 2), and as the maximum swarming rate of an A^+S^+ strain is 1.6 μm min^{-1} whereas the sum of the maximum rates of the two engines acting alone is only 1.0 μm min^{-1} [0.4 (A^-S^+) + 0.6 (A^+S^-)][34,45]. This synergism also indicates that polarity reversal of one engine is correlated with reversal of the other engine. In a movie of cells gliding on agar, cells reversing and laying down a slime trail can be seen (see Online Movie).

C-signal transduction and movement in myxococci. *Myxococcus* uses two cell-to-cell signals that have been chemically identified: the A- and C-signals. The A-signal is a QUORUM SENSOR for an early stage of development. The C-signal is a 17-kDa cell-surface protein, and is only transmitted by end-to-end contact with another cell[13,46,47]. The C-signal is found on the surface of myxobacterial cells and is processed from the protein product of *csgA* by a cell-surface protease[12]. It is neither observed, nor expected, to be diffusible. The C-signal orchestrates morphogenesis of the fruiting body, not by chemotaxis, but by modifying the movement behaviour of cells. Finally, the C-signal induces the cells to differentiate spores. The proteins of the *act* operon respond

QUORUM SENSOR
An extracellular signal molecule, the concentration of which is proportional to the cell concentration, and which is used by many bacteria to detect cell density

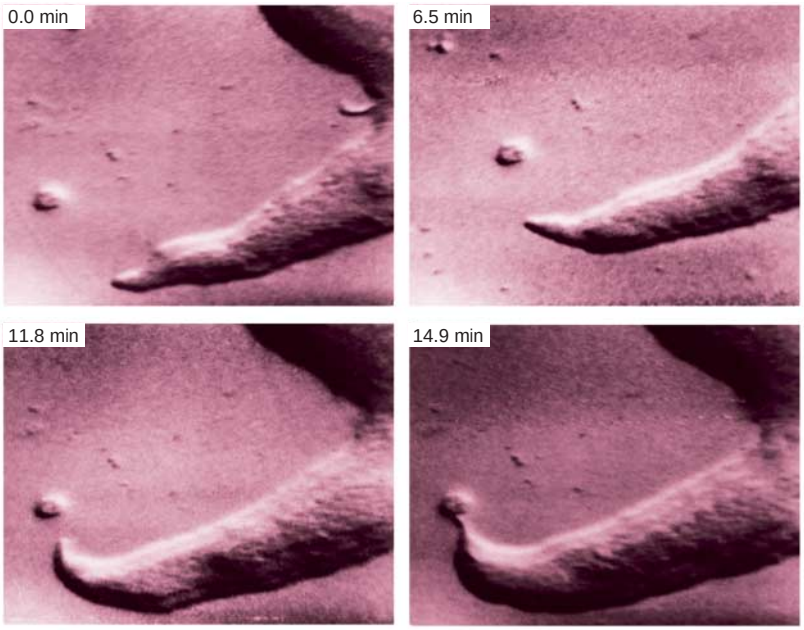

Figure 5 | **The directing effect of elasticotaxis on a *Myxoccocus* swarm towards a colony of prey cells.** Reproduced with permission from REF. 44 © (1983) American Society for Microbiology.

to the C-signal by activating transcription of the *csgA* gene (FIG. 6) (REFS 48,49; T.M.A. Gronewold and D.K., manuscript in preparation). This feedback increases the number of C-signal molecules on the cell surface. After each signalling event, positive feedback adds more C-signal molecules to the cell surface. Beginning at 3 hours into development, the C-signal increases from a few molecules on each average cell to several hundred molecules at the time of sporulation.

The contact-dependent C-signal transduction circuit is shown in FIG. 6. For some time, the FruA response regulator has been known to be important for sporulation[50]. Ellehauge and Søgaard-Andersen

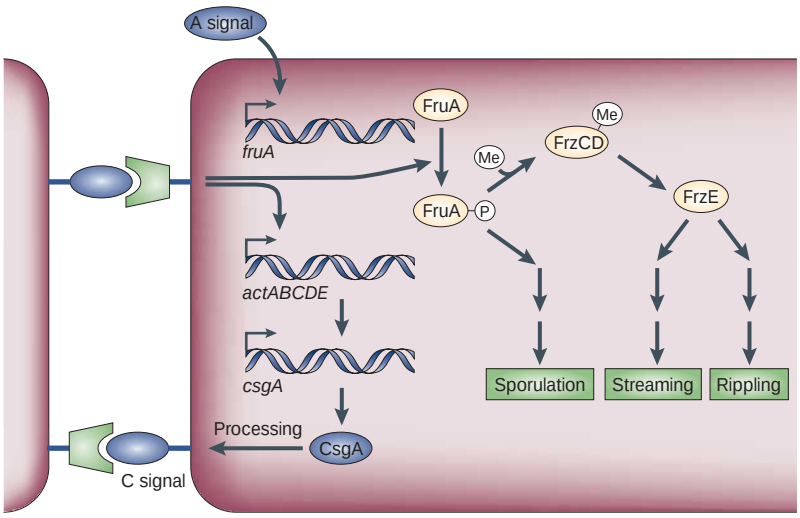

Figure 6 | **The C-signal transduction circuit.** Two cells are shown signalling to each other and both have the same transduction circuit but, for clarity it is shown only in the cell on the right. Evidence for the circuit is detailed in REFS 61,64. Frz, frizzy; Me, methyl. Modified with permission from REF. 64 © (2000) National Academy of Sciences.

have since furthered our understanding and shown that C-signal reception can induce post-translational modification (probably phosphorylation) of FruA[51]. Aggregation was also found to be impaired in a *fruA* transposon insertion mutant[52].

The myxobacterial frizzy (Frz) proteins have sequences similar to those of proteins that are involved in the *Escherichia coli* and *Salmonella enterica* serovar Typhimurium chemosensory signal-transduction pathway[53]. Null mutations in *frz* genes have a weak S^- phenotype that is probably related to a defect in reversal control[43]. In *M. xanthus*, the first protein of the *frz* cascade is the FrzCD protein, a methyl-accepting chemosensory protein (MCP). However, in contrast to the enteric chemotaxis system, FrzCD is a cytoplasmic protein rather than a membrane receptor. Frz proteins modulate reversals in growing cells; cells usually reverse once every 10 min on average, and apparently at random. Null *frz* mutants either decrease the reversal frequency to once every 100 min (for example, Δ*frzC*) or increase it to several each min (only Δ*frzD*). Methylation and demethylation of FrzCD are catalysed by FrzF and FrzG; mutation of *frzF* decreases the reversal frequency whereas mutation of *frzG* increases the frequency[54]. In the stationary phase of growth, about half of the FrzCD is methylated and about half is non-methylated[11].

In response to the C-signal, FruA sets three processes in motion — waves, aggregation and sporulation (FIG. 6). Reception of the (low) initial number of C-signal molecules in each cell activates the Frz two-component system by phosphorylation of FruA. The cell's response is to glide first in one direction, then, periodically, to reverse its direction. It is this response to the C-signal that gives rise to the wave pattern, which is also called rippling[7,55].

Travelling waves. Organized, travelling waves of cells occur early and in random areas of a developing myxococcal culture[56,57]. They are the first movement pattern in development in which reversals are regulated. Using green fluorescent protein (GFP), the movements of individual cells forming a wave pattern have been tracked[55], and the tracked cells were seen to move back and forth in the direction of wave propagation. This periodicity arises from cell reversals that occur when two counter-migrating waves collide[46]. Although the cells are constrained to move in the direction of wave propagation, the trajectory of every tracked cell was different. Some reversals were seen in the troughs and ahead of or behind a crest. FOURIER ANALYSIS detected a period that is specific to cells making waves and which is only found in movement on the axis of wave propagation that is superimposed on random reversals[55]. The Fourier period is 8 min, which is approximately equal to the period of the macroscopic waves (8.2 ± 0.6 min)[55]. Moreover, the speed of wave propagation is 5.5 ± 0.3 μm min^{-1}, which corresponds to the measured speed at which the A^+S^+ cells glide (approximately one cell length each min). Mathematical simulation has shown the pathway that is illustrated in FIG. 6 to be sufficient to account for travelling waves (BOX 3).

Box 3 | Mathematical models of travelling waves

In response to the initial low level of the C-signal, myxobacterial cells begin to glide, periodically reversing direction. To test whether this is sufficient to explain the travelling waves, the regulatory pathway that is shown in FIG. 6 has been simulated using simultaneous partial differential equations[58]. The model also included the assumptions that each cell has a reversal clock (still to be identified biochemically), and is refractory for a short time after receiving the C-signal. With these modifications, the model did simulate travelling waves, including the random reversals[55].

In addition, the model explained several puzzling observations. First, that even after hours of wave motion, there is no net transport of cells by the waves. This follows from the model because individual cells are shuttling back and forth. Second, the waves, which are dense heaps of cells[57], seem to interpenetrate after intersection. This is not the case; collisions between counter-migrating cells in two wave crests lead them to transmit the C-signal to each other and, in response, reverse their direction of movement and appear to reflect from each other[46]. Consequently, the shape of a wave passes through an intersection, but the cells themselves do not. Finally, the model makes the quantitative prediction that the wavelength should be twice the average cell velocity multiplied by the wave period[52]. Indeed, the measured wavelength of 91 ± 8 μm does equal [(2 x 5 μm min^{-1}) x 8.2 ± 0.6 min]. Although there is as yet no independent evidence for a clock and a refractory period, two other wave simulations by cellular automaton models have been found to require a post-signalling refractory period to sustain waves[74,75].

Stages of aggregation. The main stages of aggregation in submerged agar culture (SAC) are shown in FIG. 7 (D. K. and R. Welch, manuscript in preparation;). At 0 min (FIG. 7a), the dense culture has a uniform density; ~10^7 cells are equally distributed in the visible sector of the spot. However, at 206 min (FIG. 7b), the culture is no longer homogeneous and a grey band appears, indicating that the cell density is higher in this band; aggregates of cells form at the edge of the band. In general, fruiting-body aggregates, both on agar and in submerged culture, initiate at sites of higher-than-average cell density (D. K. and R. Welch, manuscript in preparation). In SAC, the initial aggregates are regularly spaced at intervals of one wavelength (FIG. 7c).

A separation of one wavelength offers a strong indication to the mechanism of aggregation. Aggregates are found at all the intersections between a left-moving wave crest, a right-moving wave crest and the peripheral band of high cell density. Given that the waves comprise piles of cells, such intersections have more cells than anywhere else in the culture. The intersections are illustrated in FIG. 7f. Why do cells in moving waves stop and aggregate at these triple intersections? I suggest that the cells must stop when, arriving from opposite directions, they collide with each other and with the cells packed at high density in the peripheral band. An analogy would be many motor cars arriving on a road from several directions — effectively, the cells find themselves stuck in a 'traffic jam'. However, unlike traffic jams on roads, these cellular traffic jams have three dimensions because cells can enter them at many different levels. The jam is a mass of cells in which each one blocks the movement of the others. Consider the A- and S-engines, described above, trying to 'drive' their cell forward in a three-dimensional jam of many cells. Such are the mechanics of the A-engine[40] and the S-engine[23] that both would be expected to stall when one cell bumps into a stationary cell. The traffic jams in SAC are almost spherical (FIG. 7c–e).

Traffic jams are also found in Kuner submerged culture, which is like SAC but without agar (FIG. 8a). They are not spherical, but instead are flat and elongated. Waves are not seen in such cultures, but there are intersections of adjacent domains in the initial facet pattern of cells, and this is where jams form (REF. 59; D.K. and R. Welch, manuscript in preparation). Like the spherical traffic jams in FIG. 7, the flat traffic jams shown in FIG. 8 remain stationary for several hours. A high-magnification scanning electron microscope (EM) view of a jam in FIG. 8a shows cells entering from all sides. Phase-contrast, light microscope images show the jam to be a dense patch of cells resting on the flat sheet of cells that covers the bottom of the culture dish (D. K. and R. Welch, manuscript in preparation). Like the traffic jams in SAC, these traffic jams remain in place for many hours because the cells are blocking each other's movement.

The traffic jams in SAC enlarge as waves wash over them and deposit more cells, or shrink as cells from the surface of the jam leave the aggregate and return to the travelling waves. The waves are unfocused at 678 min[58] (FIG. 7c), this is in contrast to the sharp crosses at 1,924 min (FIG. 7d). Similarly, in Kuner submerged culture, some of the traffic jams enlarge as cells enter from their surroundings (D. K. and R. Welch, manuscript in preparation).

The traffic jam halts the forward motion of the cells for several hours. As both the A- and S-engines were 'running' before the cells 'stalled', as soon as the cells find paths through the jam by turning to avoid the blocking cells, they begin to move (D. K. and R. Welch, manuscript in preparation). When the cells move within the aggregate, they frequently make end-to-end contact with other cells and they transmit the C-signal to each other. Repeated C-signalling in the travelling waves increases the number of C-signal molecules on the cell surface owing to the *act* positive-feedback loop (FIG. 6). The higher level of signal flowing through the FruA response regulator and the Frz chemosensory pathway reaches the threshold for a streaming response, as indicated in FIG. 6. The fact that waves depend on a low C-signal-specific activity is shown by the Δ*actA* and Δ*actB* mutants. These mutants can produce the C-signal, but they cannot increase the amount of C-signal that is present on the cell surface, and they remain in wave mode for days, rather than the usual hours[48]. Jelsbak and Søgaard-Andersen have tracked streaming cells and have demonstrated that the C-signal induces both a

FOURIER ANALYSIS
Mathematical decomposition of a complex periodic function into a sum of simple sine waves.

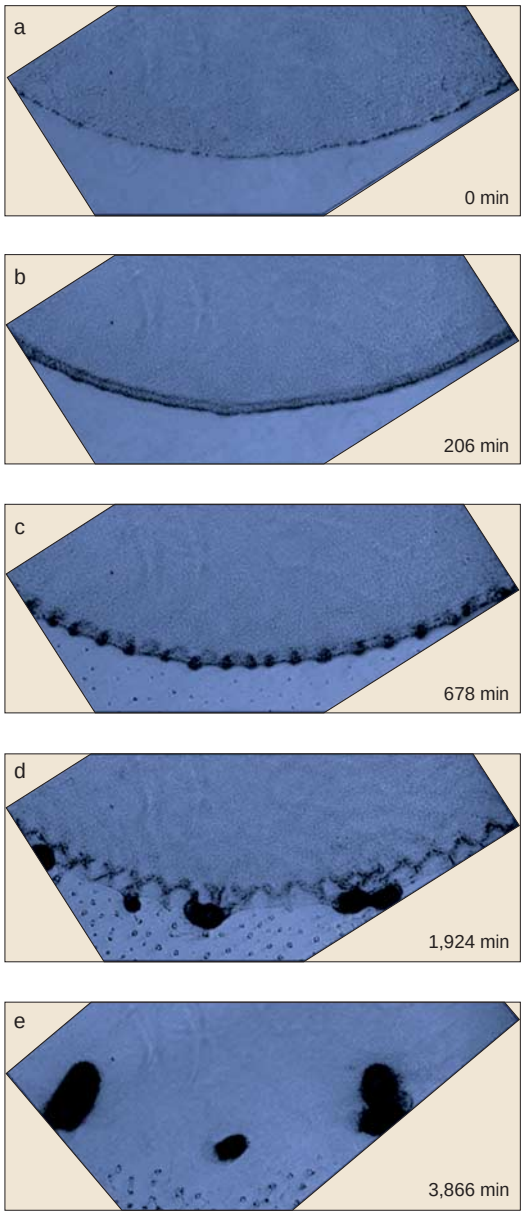

f **Stationary aggregates form at triple intersections**

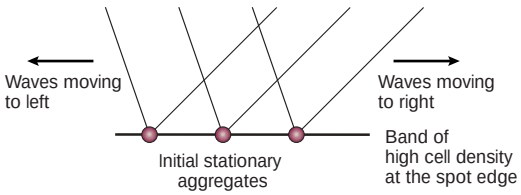

Figure 7 | **Fruiting-body aggregation in submerged agar culture.** Time-lapse images were collected at 1.5-min intervals from a culture maintained at 25 °C with a heated stage. Phase-contrast images were collected through a ×10 objective lens and captured on a charge-coupled device (CCD) camera[55]. The time from the initiation of development is shown in the lower right-hand corner of frames **a**–**e**. The next frame (**f**) shows the formation of aggregates at the intersection of three ridges of high cell density: the peripheral band and two, counter-migrating wave crests.

decrease in reversal frequency and an increase in speed[60,61] — a very different reversal pattern from that found in waves.

A model for streaming behaviour is shown in FIG. 8b. The cells turn to break the initial jam, and begin to stream as a result of C-signalling. This motility becomes apparent when adjacent aggregates begin to fuse with each other. The changes in individual stationary aggregates and their fusion can be followed in FIG. 7. At 1,924 min (FIG. 7d), two pairs of aggregates have bi-lobate shapes because they are undergoing fusion. As two of these aggregates were themselves the products of a previous fusion, they fuse to give a structure four times the size of an initial aggregate. Fusion builds large aggregates the size of mature fruiting bodies. Fusion is seldom observed in Kuner-type submerged culture because the traffic jams are farther apart than in SAC (D. K. and R. Welch, manuscript in preparation). The ability of aggregates to fuse strongly indicates that cells are streaming around inside the aggregate in closed loops. Sager has tracked cells at the bottom of a nascent fruiting body on agar and observed them moving in circular paths — half the cells moving clockwise and half moving anti-clockwise[62]. Additionally, O'Connor and Zusman reported spiral arrangements of cells within fruiting bodies[63].

Sporulation. In a mounded and motile aggregate (such as in FIG. 7e and BOX 1; known as a 'Kuner fruiting body'), the cell density is high, and the cells are flowing in cyclic paths. I propose that these cells are moving like logs flowing in a river, which nudge each other end-to-end and so can transmit the C-signal to each other. The cells undergo many more episodes of C-signalling, and sustain more *act*-mediated positive feedback. Finally, the number of C-signal molecules on the cell surface is ~100-fold above the level found at the time of the travelling wave pattern. Like wave formation and streaming, sporulation has its own C-signal threshold. Spore formation is induced inside the fruiting body because it is only in this large elliptical aggregate that the level of the C-signal rises above the required threshold[64]. So, spore differentiation is induced in the fruting body, where the spores are poised for subsequent dispersal[65]. Restricting spore formation to the fruiting body might be the biological mechanism for evolution of the C-signal response system. Cells that remain outside of the fruiting body, called peripheral rods, have fewer C-signal molecules per cell[64], and they never sporulate[66].

Conclusion

This is an exciting time for investigators of myxobacteria. *M. xanthus* has ~7,500 genes and, at present is the largest bacterial genome. Are so many genes needed to coordinate its multicellular activities? Are many genes needed for a diverse secondary metabolism? Answers to these questions are expected at the end of 2003, with the publication of the complete, annotated genome sequence of *M. xanthus*. Some findings in *Myxococcus* might be extrapolated to other gliding or twitching bacteria (BOX 2). Myxobacteria are models

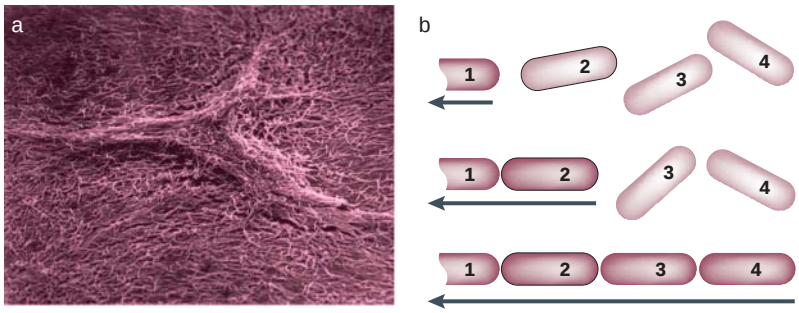

Figure 8 | **A traffic jam and streaming in the construction of fruiting bodies in submerged agar culture. a** | A scanning electron micrograph of a DK1622 aggregate 8 hours into development[59]. **b** | A model for the C-signal induction of streams. C-signalling by end-to-end contact results in sequential recruitment of cells to chains of moving cells. Arrows indicate the direction of movement of chains of cells. Dark cells indicate cells that have been recruited to a chain and are actively C-signalling. Light cells are competent for C-signalling, but are not yet engaged in C-signalling. Moving to the left, cell 2 makes end-to-end contact with cell 1, which is already moving to the left. The two cells signal to each other, and both respond by increasing their speed and continuing to move in the direction they had been moving[11]. Cells 3 and 4, moving at random, are sequentially recruited in the same way as cell 2.

not only for cell movement, but also for organized movement and morphogenesis. Until now, most models of morphogenesis in vertebrate animals have taken their cue from the activity of cyclic AMP in *Dictyostelium discoideum*, and have postulated diffusible morphogens. However, cell-contact signals are also important. Vertebrate long bones are laid down early in development by the organized movements of cells. These cells then pass signals to each other, and initiate their programmes of cell differentiation — essentially the same scheme that is used by myxobacteria to construct their spore-containing fruiting bodies. Many different fruiting body shapes occur among the 40 species of myxobacteria, demonstrating the versatility of cell-contact signalling. The shape of the *M. xanthus* fruiting body, including the location of its spores, depends on a cell-contact signal. Recent studies of Wnt signalling in mammals[67] show that the arrangement of cells and local cell-to-cell signalling must be taken into account. Myxobacteria offer ready experimental access to the formation of such patterns.

1. Reichenbach, H. in *The Myxobacteria* (ed. Rosenberg, E.) 1–50 (Springer–Verlag, New York, 1984).
2. Rosenberg, E., Keller, K. H. & Dworkin, M. Cell density-dependent growth of *Myxococcus xanthus* on casein. *J. Bacteriol.* **129**, 770–777 (1977).
3. Reichenbach, H. in *Myxobacteria II* (eds Dworkin, M. & Kaiser, D.) 13–62 (ASM Press, Washington DC, 1993).
4. Burchard, R. P. Gliding motility mutants of *Myxococcus xanthus*. *J. Bacteriol.* **104**, 940–947 (1970).
5. Kaiser, D. in *The Myxobacteria* (ed. Rosenberg, E.) 163–184 (Springer–Verlag, New York, 1984).
6. Hagen, D. C., Bretscher, A. P. & Kaiser, D. Synergism between morphogenetic mutants of *Myxococcus xanthus*. *Dev. Biol.* **64**, 284–296 (1978).
7. Kim, S. K. & Kaiser, D. C-factor: a cell-cell signalling protein required for fruiting-body morphogenesis of *M. xanthus*. *Cell* **61**, 19–26 (1990).
8. Kuspa, A., Plamann, L. & Kaiser, D. Identification of heat-stable A-factor from *Myxococcus xanthus*. *J. Bacteriol.* **174**, 3319–3326 (1992).
9. Plamann, L., Kuspa, A. & Kaiser, D. Proteins that rescue A-signal-defective mutants of *Myxococcus xanthus*. *J. Bacteriol.* **174**, 3311–3318 (1992).
10. Kim, S. K. & Kaiser, D. Purification and properties of *Myxococcus xanthus* C-factor, an intercellular signaling protein. *Proc. Natl Acad. Sci. USA* **87**, 3635–3639 (1990).
11. Søgaard-Andersen, L. & Kaiser, D. C-factor, a cell-surface-associated intercellular signaling protein, stimulates the cytoplasmic Frz signal transduction system in *Myxococcus xanthus*. *Proc. Natl Acad. Sci. USA* **93**, 2675–2679 (1996).
12. Søgaard-Andersen, L. Coupling gene expression and multicellular morphogenesis during fruiting body formation in *Myxococcus xanthus*. *Mol. Microbiol.* **48**, 1–8 (2003).
13. Kim, S. K. & Kaiser, D. Cell alignment required in differentiation of *Myxococcus xanthus*. *Science* **249**, 926–928 (1990).
14. McBride, M. J., Hartzell, P. & Zusman, D. R. in *Myxobacteria II* (eds Dworkin, M. & Kaiser, D.) 285–305 (ASM Press, Washington DC, 1993).
15. Hodgkin, J. & Kaiser, D. Genetics of gliding motility in *M. xanthus* (Myxobacterales): genes controlling movement of single cells. *Mol. Gen. Genet.* **171**, 167–176 (1979).
16. Hodgkin, J. & Kaiser, D. Genetics of gliding motility in *M. xanthus* (Myxobacterales): two gene systems control movement. *Mol. Gen. Genet.* **171**, 177–191 (1979).
17. Maier, B., Potter, L., So, M., Seifert, H. S. & Sheetz, M. P. Single pilus motor forces exceed 100 pN. *Proc. Natl Acad. Sci. USA* **99**, 16012–16017 (2002).
18. Kaiser, D. Social gliding is correlated with the presence of pili in *Myxococcus xanthus*. *Proc. Natl Acad. Sci. USA* **76**, 5952–5956 (1979).
19. Wu, S. S. & Kaiser, D. Regulation of expression of the *pilA* gene in *Myxococcus xanthus*. *J. Bacteriol.* **179**, 7748–7758 (1997).
20. Wall, D., Kolenbrander, P. E. & Kaiser, D. The *Myxococcus xanthus pilQ* (*sglA*) gene encodes a secretin homolog required for type IV pili biogenesis, S motility and development. *J. Bacteriol.* **181**, 24–33 (1999).
21. Wolfgang, M. *et al.* PilT mutations lead to simultaneous defects in competence for natural transformation and twitching motility in piliated *Neisseria gonorrhoeae*. *Mol. Microbiol.* **29**, 321–330 (1998).
22. Vale, R. D. AAA proteins: lords of the ring. *J. Cell Biol.* **150**, F13–F19 (2000).
23. Merz, A. J., So, M. & Sheetz, M. P. Pilus retraction powers bacterial twitching motility. *Nature* **407**, 98–102 (2000). **Describes the use of laser tweezers to directly measure the force of the type IV pilus retraction.**
24. Merz, A. J. & Forest, K. T. Bacterial surface motility: slime trails, grappling hooks and nozzles. *Curr. Biol.* **12**, R297–R303 (2002).
25. Sun, H., Zusman, D. R. & Shi, W. Type IV pilus of *Myxococcus xanthus* is a motility apparatus controlled by the *frz* chemosensory system. *Curr. Biol.* **10**, 1143–1146 (2000).
26. Kaiser, D. How do pili pull? *Curr. Biol.* **10**, R777–R780 (2000).
27. Skerker, J. & Berg, H. Direct observation of extension and retraction of type IV pili. *Proc. Natl Acad. Sci. USA* **98**, 6901–6904 (2001).
28. Wall, D. & Kaiser, D. Type IV pili and cell motility. *Mol. Microbiol.* **32**, 1–10 (1999).
29. Arnold, J. W. & Shimkets, L. J. Cell surface properties correlated with cohesion in *Myxococcus xanthus*. *J. Bacteriol.* **170**, 5771–5777 (1988).
30. Arnold, J. W. & Shimkets, L. Inhibition of cell–cell interactions in *Myxococcus xanthus* by congo red. *J. Bacteriol.* **170**, 5765–5770 (1988).
31. Behmlander, R. M. & Dworkin, M. Biochemical and structural analyses of the extracellular matrix fibrils of *Myxococcus xanthus*. *J. Bacteriol.* **176**, 6295–6303 (1994).
32. Dworkin, M. Fibrils as extracellular appendages of bacteria: their role in contact-mediated cell–cell interactions in *Myxococcus xanthus*. *BioEssays* **21**, 590–595 (1999).
33. Yang, Z. *et al.* The *Myxococcus xanthus dif* genes are required for the biogenesis of cell surface fibrils essential for social gliding motility. *J. Bacteriol.* **182**, 5793–5798 (2000).
34. Kaiser, D. & Crosby, C. Cell movement and its coordination in swarms of *Myxococcus xanthus*. *Cell Motil.* **3**, 227–245 (1983).
35. Bowden, M. G. & Kaplan, H. B. The *Myxococcus xanthus* lipopolysaccharide O-antigen is required for social motility and multicellular development. *Mol. Microbiol.* **30**, 275–284 (1998).
36. Li, Y. *et al.* Extracellular polysaccharides mediate pilus retraction during social motility of *Myxococcus xanthus*. *Proc. Natl Acad. Sci. USA* **100**, 5443–5448 (2003).
37. Kuhlwein, H. & Reichenbach, H. *Schwarmentwicklung und Morphogenese bei Myxobacterien–Archangium, Myxococcus, Chondrococcus, Chondromyces.* (eds Heunert, H. H. & Kuczka, H.) Film C893 (Inst. Wissensch. Film, Gottingen, Germany, 1965).
38. Burchard, R. P. Trail following by gliding bacteria. *J. Bacteriol.* **152**, 495–501 (1982).
39. Shi, W. & Zusman, D. R. The two motility systems of *Myxococcus xanthus* show different selective advantages on various surfaces. *Proc. Natl Acad. Sci. USA* **90**, 3378–3382 (1993).
40. Wolgemuth, C., Hoiczyk, E., Kaiser, D. & Oster, G. How myxobacteria glide. *Curr. Biol.* **12**, 1–20 (2002). **Provides experimental evidence for the secretion of slime from jets at the rear of *M. xanthus* cells that propels them for A-motility.**
41. Hoiczyk, E. & Baumeister, W. The junctional pore complex, a prokaryotic secretion organelle, is the molecular motor underlying gliding motility in cyanobacteria. *Curr. Biol.* **8**, 1161–1168 (1998).
42. Stanier, R. Y. Elasticotaxis in myxobacteria. *J. Bacteriol.* **44**, 405–412 (1942).
43. Fontes, M. & Kaiser, D. *Myxococcus* cells respond to elastic forces in their substrate. *Proc. Natl Acad. Sci. USA* **96**, 8052–8057 (1999).
44. Dworkin, M. Tactic behavior of *Myxococcus xanthus*. *J. Bacteriol.* **154**, 452–459 (1983).
45. Burchard, R. P. Growth of surface colonies of the gliding bacterium *Myxococcus xanthus*. *Arch. Microbiol.* **96**, 247–254 (1974).
46. Sager, B. & Kaiser, D. Intercellular C-signaling and the traveling waves of *Myxococcus*. *Genes Dev.* **8**, 2793–2804 (1994).
47. Kim, S. K. & Kaiser, D. Cell motility is required for the transmission of C-factor, an intercellular signal that coordinates fruiting body morphogenesis of *Myxococcus xanthus*. *Genes Dev.* **4**, 896–905 (1990).
48. Gronewold, T. M. A. & Kaiser, D. The *act* operon controls the level and time of C-signal production for *M. xanthus* development. *Mol. Microbiol.* **40**, 744–756 (2001). **Provides evidence for a positive feedback circuit that increases the number of C-signal molecules that are displayed on the cell surface.**
49. Gronewold, T. M. A. & Kaiser, D. *act* operon control of developmental gene expression in *Myxococcus xanthus*. *J. Bacteriol.* **184**, 1172–1179 (2002).
50. Ogawa, M., Fujitani, S., Mao, X., Inouye, S. & Komano, T. FruA, a putative transcription factor essential for the development of *Myxococcus xanthus*. *Mol. Microbiol.* **22**, 757–767 (1996).
51. Ellehauge, E., Norregaard-Madsen, M. & Søgaard-Andersen, L. The FruA signal transduction protein provides a checkpoint for the temporal coordination of intercellular signals in *M. xanthus* development. *Mol. Microbiol.* **30**, 807–813 (1998). **References 50 and 51 show that the *fruA* response-regulator links reception of the C-signal to the *frz* chemosensory pathway.**
52. Søgaard-Andersen, L., Slack, F., Kimsey, H. & Kaiser, D. Intercellular C-signaling in *Myxococcus xanthus* involves a

branched signal transduction pathway. *Genes Dev.* **10**, 740–754 (1996).
53. McBride, M. J., Weinberg, R. A. & Zusman, D. R. Frizzy aggregation genes of the gliding bacterium *Myxococcus xanthus* show sequence similarities to the chemotaxis genes of enteric bacteria. *Proc. Natl Acad. Sci. USA* **86**, 424–428 (1989).
54. McCleary, W. R., McBride, M. J. & Zusman, D. R. Developmental sensory transduction in *Myxococcus xanthus* involves methylation and demethylation of *frzCD*. *J. Bacteriol.* **172**, 4877–4887 (1990).
55. Welch, R. & Kaiser, D. Cell behavior in traveling wave patterns of myxobacteria. *Proc. Natl Acad. Sci. USA* **98**, 14907–14912 (2001).
56. Reichenbach, H. Rhythmic motion in swarms of myxobacteria. *Ber. Deutsch. Bot. Ges.* **78**, 102–105 (1965).
57. Shimkets, L. & Kaiser, D. Induction of coordinated movement of *Myxococcus xanthus* cells. *J. Bacteriol.* **152**, 451–461 (1982).
58. Igoshin, O., Mogilner, A., Welch, R., Kaiser, D. & Oster, G. Pattern formation and traveling waves in myxobacteria: theory and modeling. *Proc. Natl Acad. Sci. USA* **98**, 14913–14918 (2001).
59 Kuner, J. & Kaiser, D. Fruiting body morphogenesis in submerged cultures of *Myxococcus xanthus*. *J. Bacteriol.* **151**, 458–461 (1982).
60. Jelsbak, L. & Søgaard-Andersen, L. The cell-surface associated C-signal induces behavioral changes in individual *M. xanthus* cells during fruiting body morphogenesis. *Proc. Natl Acad. Sci. USA* **96**, 5031–5036 (1999).
61. Jelsbak, L. & Søgaard-Andersen, L. Pattern formation by a cell-surface associated morphogen in *M. xanthus*. *Proc. Natl Acad. Sci. USA* **99**, 2032–2037 (2002).
The first cell-tracking experiments of cells that are induced to stream by the C-signal.
62. Sager, B. & Kaiser, D. Two cell-density domains within the *Myxococcus xanthus* fruiting body. *Proc. Natl Acad. Sci. USA* **90**, 3690–3694 (1993).
63. O'Connor, K. A. & Zusman, D. R. Patterns of cellular interactions during fruiting-body formation in *Myxococcus xanthus*. *J. Bacteriol.* **171**, 6013–6024 (1989)
64. Julien, B., Kaiser, D. & Garza, A. Spatial control of cell differentiation in *Myxococcus xanthus*. *Proc. Natl Acad. Sci. USA* **97**, 9098–9103 (2000).
The first paper to show that the C-signal induces sporulation only inside of a fruiting body.
65. O'Connor, K. A. & Zusman, D. R. Behavior of peripheral rods and their role in the life cycle of *Myxococcus xanthus*. *J. Bacteriol.* **173**, 3342–3355 (1991).
66. Kaiser, D. Cell fate and organogenesis in bacteria. *Trends Genet.* **15**, 273–277 (1999).
67. Willert, K. *et al*. Wnt proteins are lipid-modified and can act as stem cell growth factors. *Nature* **423**, 448–452 (2003).
68 Henrichsen, J. Bacterial surface translocation: a survey and a classification. *Bacteriol. Rev.* **36**, 478–503 (1972).
69. Henrichsen, J. Twitching motility and its mechanism. *Acta Path. Microbiol. Scand.* **83**, B187–B190 (1975).
70. Mattick, J. S. Type IV pili and twitching motility. *Annu. Rev. Microbiol.* **56**, 289–314 (2002).
71. Bieber, D. *et al.* Type IV pili, transient bacterial aggregates and virulence in enteropathogenic *Escherichia coli*. *Science* **280**, 2114–2118 (1998).
72. O'Toole, G. A. & Kolter, R. Initiation of biofilm formation in *Pseudomonas fluorescens* WCS365 proceeds via multiple, convergent signalling pathways: a genetic analysis. *Mol. Microbiol.* **28**, 449–461 (1998).
73. Klausen, M. Biofilm formation by *Pseudomonas aeruginosa* wild type, flagella and type IV pili mutants. *Mol. Microbiol.* **48**, 1511–1524 (2003).
74. Börner, U., Deutsch, A., Reichenbach, H. & Bär, M. Rippling patterns in aggregates of myxobacteria arise from cell–cell collisions. *Phys. Rev. Lett.* **89**, 078101 (2002).
75. Alber, M. S., Jiang, Y. & Kiskowski, M. Lattice gas cellular automata model for rippling and aggregation in myxobacteria. *SIAM J. Appl. Math.* (in the press).

Acknowledgements
I thank L. Jelsbak, O. Igoshin, G. Oster and M. Alber for their suggestions. D. K. is supported by a grant from the National Institute of General Medical Sciences.

Online links

FURTHER INFORMATION
Dale Kaiser's laboratory:
http://cmgm.stanford.edu/~kaiserla/index.html
TIGR: http://www.tigr.org/
Access to this interactive links box is free online.